QUASAR

Quantum States: Analysis and Realizations

Start date: 1 January 2012
Duration: 24 months

chist-era

Goals

QUASAR

efficient quantum computation and communication

→ significantly improved comprehension of the underlying principles of quantum physics

→ scalable analysis tools to study the dynamics, decoherence, as well as the applicability of (large) quantum states

→ reliable and robust quantum technology components

Main objectives

QUASAR

The main objectives of QUASAR are thus to

- apply foundational principles of quantum physics to identify **novel protocols** for quantum communication and to optimize the efficient usage of **quantum channels**, both in theory and experiment
- develop scalable methods for **quantum state analysis** and introduce application oriented witnesses with high statistical significance and robustness against experimental imperfections
- implement these methods to analyse the dynamics and their applicability for **quantum metrology** for different decoherence models and identify possible feedback protocols to adaptively optimize metrological tasks.
- develop a new approach for the production of highly integrated and reliable **waveguide quantum circuits** and implement photonic quantum logic operation for robust manipulation of high-dimensional multiqubit states and for quantum simulation tasks.

The mair
- a ... ify

novel pr ... e
efficient u ... nent
- c ... nd

introduce
significar
- i ... heir

applicabi ... odels
and iden
metrolog
- c ... grated

and relia ... nic
quantum ... onal
multiqubi

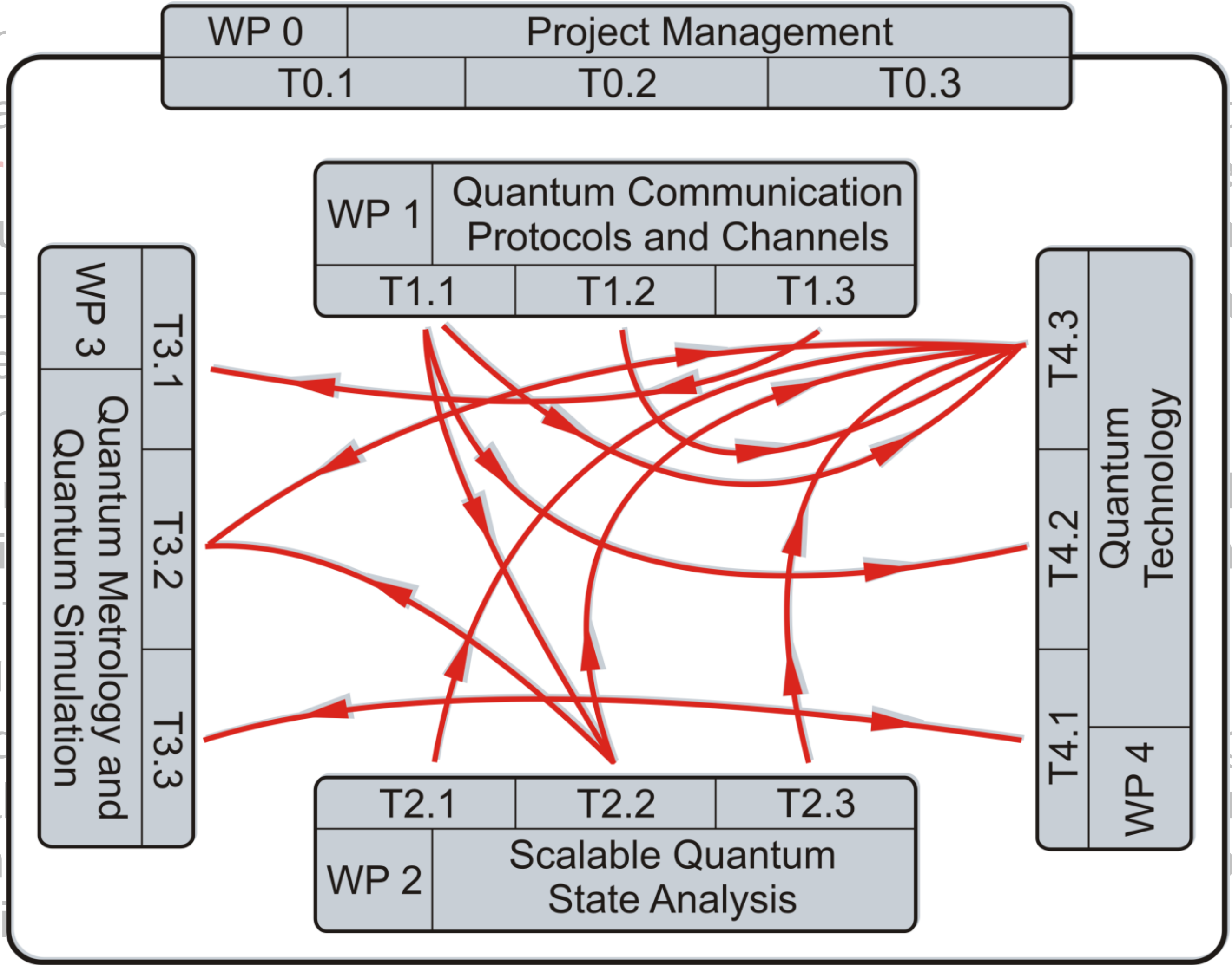

QUASAR

University of Munich

Harald Weinfurter	quantum communication
	multi-photon interferometry
LMU	foundations
Philipp Walther	quantum information processing
OEAW	foundations
Fabio Sciarrino	quantum information processing
UNIROMA1	foundations
	industrial engineering
Rafal Demkowicz	quantum metrology
Konrad Banaszek	multi-photon interferometry
UWAW	
Horodecki	multi-photon interferometry
UG	foundations
BILB	metrology
Otfried Gühne	entanglement analysis
	quantum logic
USI	foundations

s

ntry

012, duration 2 years

WP1 QC Protocols and Channels

QUASAR

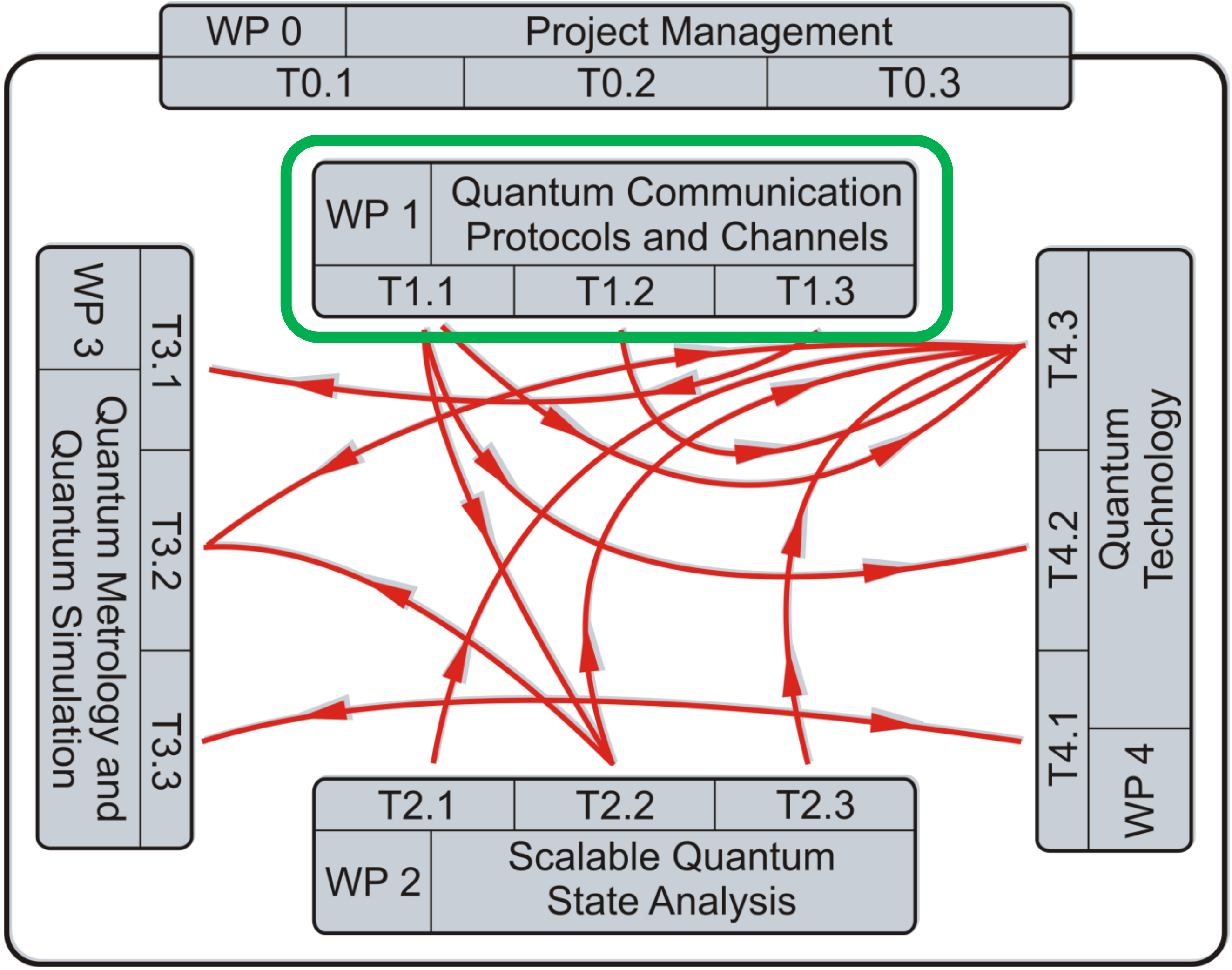

Verification of quantum computation

QUASAR

T1.1: Multipartite quantum communication and Bell theorem (OEAW)

T1.3: Quantum speed-up (OEAW)

Verification of quantum computation

- experimental interactive-proof system
- verification of the processing and the underlying quantum entanglement as resource

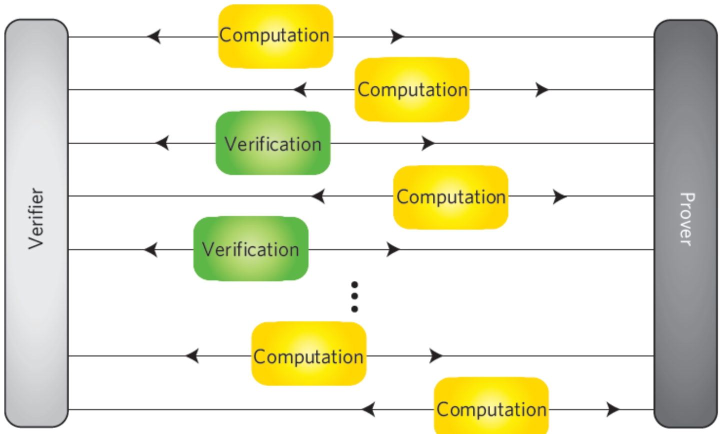

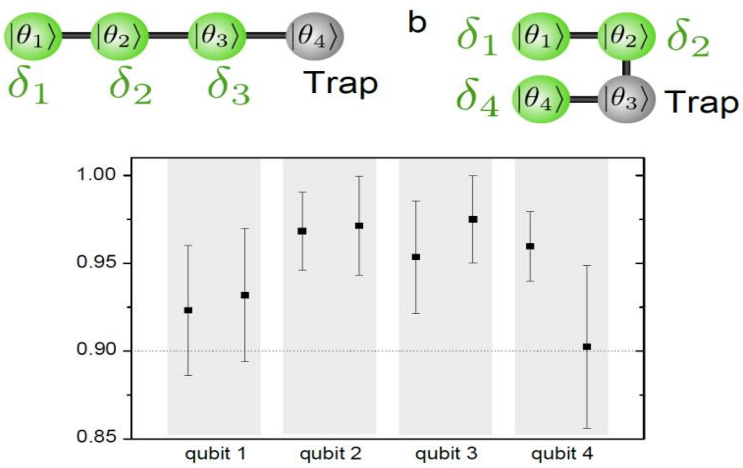

Barz, Kashefi, Fitzsimons, Walther
Nature Physics 9, 727 (2013)

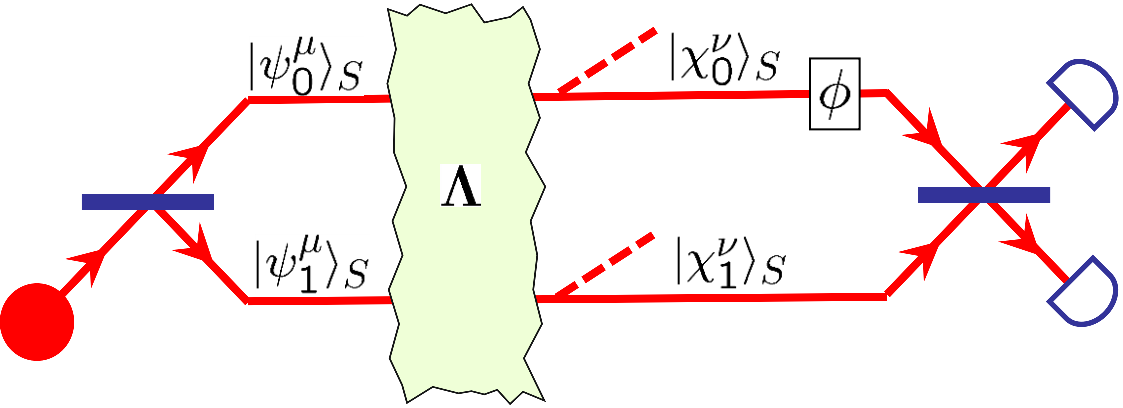

Fractional visibilities $V^{\mu\nu}$ for preparation μ and filter ν:

$$p_{\pm}^{\mu\nu}(\phi) = \frac{1}{2}[p^{\mu\nu} + \mathrm{Re}(V^{\mu\nu}e^{i\phi})]$$

Potential distinguishability of environmental states (leaking of which way information):

$$D = \tfrac{1}{2}||\widetilde{\varrho}_E'^{(1)} - \widetilde{\varrho}_E'^{(0)}|| \qquad D^2 + V_G^2 \leq 1 \qquad V_G \geq \left|\sum_{\mu\nu} \alpha_{\mu\nu} V^{\mu\nu}\right|$$

Experiment (motivated by the theory of private states): global visibility

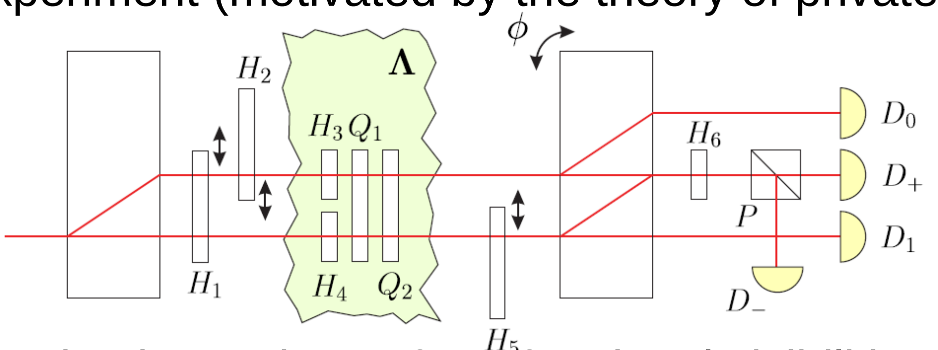

$\mu\nu$	$p^{\mu\nu}$	$V^{\mu\nu}$	$\mu\nu$	$p^{\mu\nu}$	$V^{\mu\nu}$
hh, hh	0.489	0.476	hh, vv	0.512	0.104
hv, vh	0.513	0.488	hv, hv	0.490	0.039
vh, hv	0.511	0.479	vh, vh	0.490	0.032
vv, vv	0.489	0.478	vv, hh	0.512	0.100

for mixed state input, from fractional visibilities we get: $V_G \geq 0.960 \pm 0.006$

K. Banaszek, P. Horodecki, M. Karpiński, C. Radzewicz, Nature Commun. **4**, 2594 (2013)

Lower Bounds on the Communication Complexity of Binary Local Quantum Measurement Simulation

QUASAR

→We consider communication complexity of classical simulation of bipartite correlations of local quantum measurements on systems of arbitrary dimension.
→In our scenario, we demand, that both, the correlation function and local quantum averages should be exactly simulated.
→We prove the lower bound on communication complexity of the above stated problem, which indicates, that every protocol solving the problem exactly, which has finite number of communicated bits in expectation, must have a variance, which is unbounded with respect to the size of the input of the problem (that is the dimension of a local Hilbert space).
→Our result is the first general characterization of communication complexity of the defined problem.
→We leave as an open question, whether any such protocol with finite communication in expectation exists.

Activation of entanglement in teleportation

QUASAR

→We studied the threshold amount of the classical communication required for the teleportation protocol to exceed maximal classical fidelity.

→We have shown its amount depends on the dimension of the teleported state but is, interestingly, not monotonic and reaches maximum for d = 4.

→We have also compared different classical channels of the same capacity and found that, for teleportation purposes, the one with white noise is optimal.

$$C_{min}(d, \frac{1}{d}) = \log d - (1 - \frac{1}{d}) \log(d + 1)$$

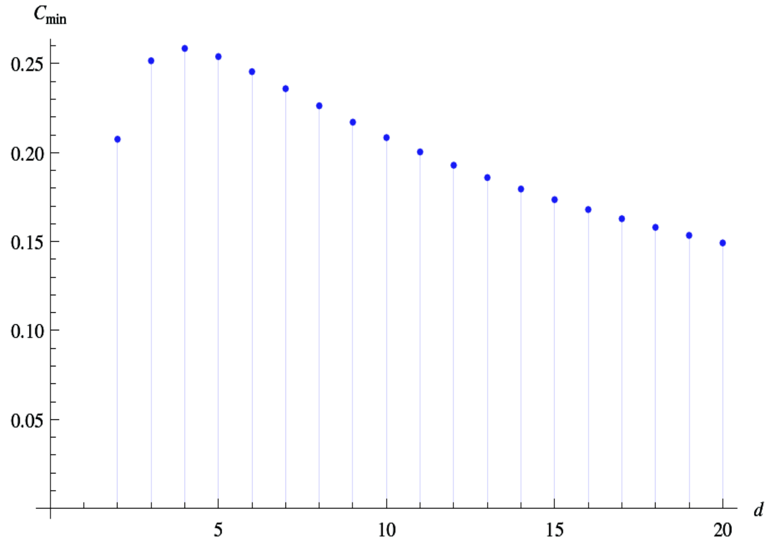

R. Weinar, W. Laskowski, M. Pawłowski, J. Phys. A 46,435301 (2013).

Entanglement witnesses with variable number of local measurements

QUASAR

→We propose a quadratic generalization of entanglement witnesses based on the formalism of correlation tensors.

→Whenever a closest separable state to the state under investigation is known, there exists an entanglement identifier, which contains squares of correlations.

→Our entanglement identifier has a form of an inequality involving only positive terms. Once the inequality is violated, entanglement of investigated state is confirmed.

→The condition often demands a few measurements, since once the inequality of the condition is violated, no further measurements are needed, since new terms can only increase the violation.

→Our condition can be used to reject inclusion in any convex set of states, e.g. PPT states, whenever the closest state from this set is known.

Genuine Multipartie Entanglement detection with Hardy Paradox

QUASAR

Standard Hardy Paradox

$$P(U_1=1,U_2=1)=q$$
$$P(U_1=1,D_2=1)=0$$
$$P(D_1=1,U_2=1)=0$$
$$P(D_1=2,D_2=2)=0$$

Our Extension

$$P(U_1=1,\ldots,U_N=1)=q$$
$$P(U_1=1,D_2=1)=0$$
$$P(U_2=1,D_3=1)=0$$
$$\ldots$$
$$P(D_1=1,U_N=1)=0$$
$$P(D_1=2,\ldots,D_N=2)=0$$

The Hardy state is unique (for qubits) and (*) must be genuinely multipartite entangled. Proof for (*): If it wasn't it could be expressed as a mixture of factorizable states (or, since it is unique for qubits, simply as a product). We find *j*, such that *j*th particle belongs to one subsystem and (*j*+1)th to the other Then

$$P(U_j=1,D_{j+1}=1)=$$
$$\underbrace{P(U_j=1)}_{>0}\underline{P(D_{j+1}=1)}=0$$

So that the state of the (*j*+1)th qubit is pure. Repeating this procedure *N*-1 times, we end up with an *N*-product state, which cannot solve the Hardy Paradox.

R. Rahaman, M. Wieśniak, M. Żukowski, arxiv.org/1303.0128

WP2 Scalable Quantum State Analysis

QUASAR

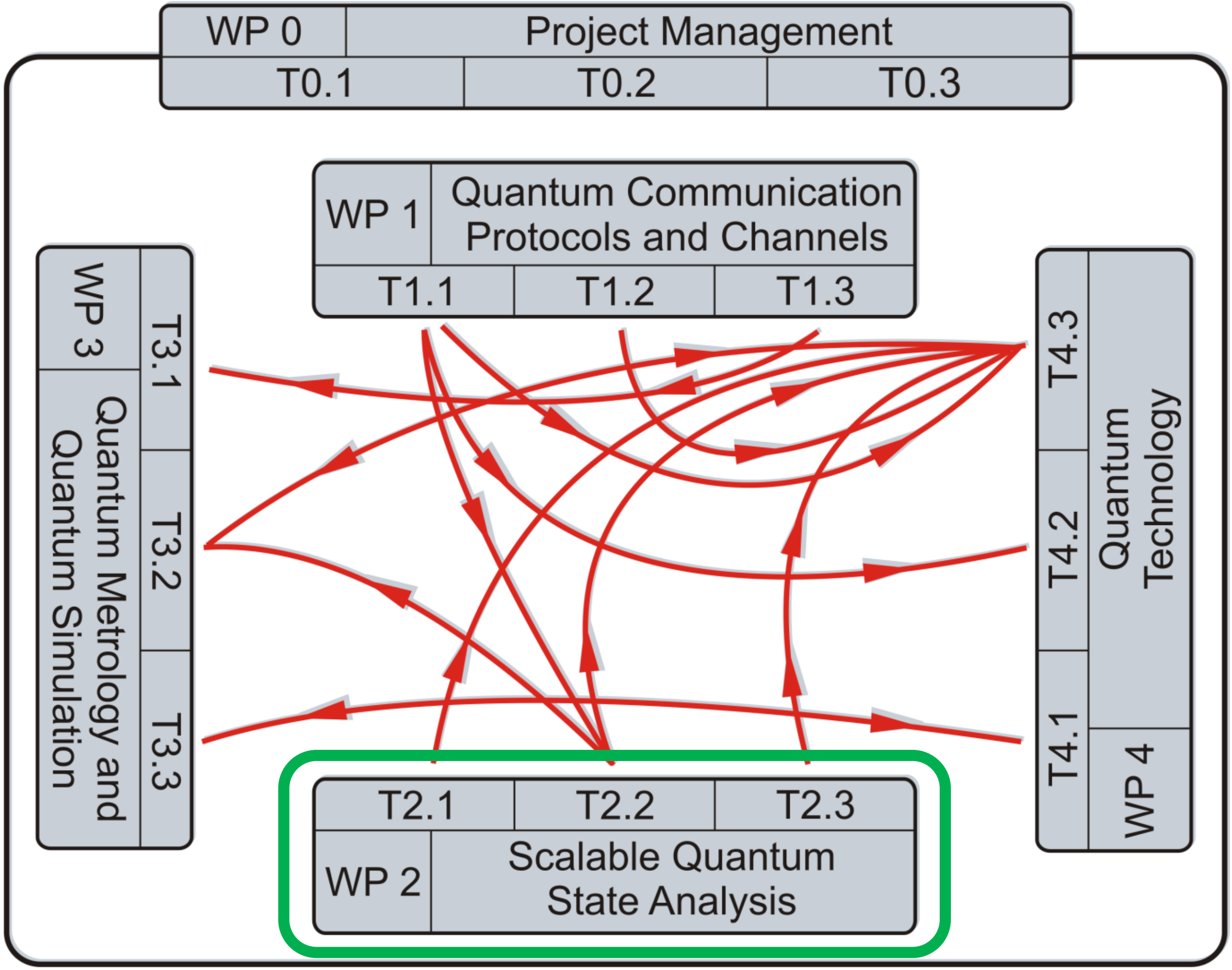

Systematic Errors – Introduction

QUASAR

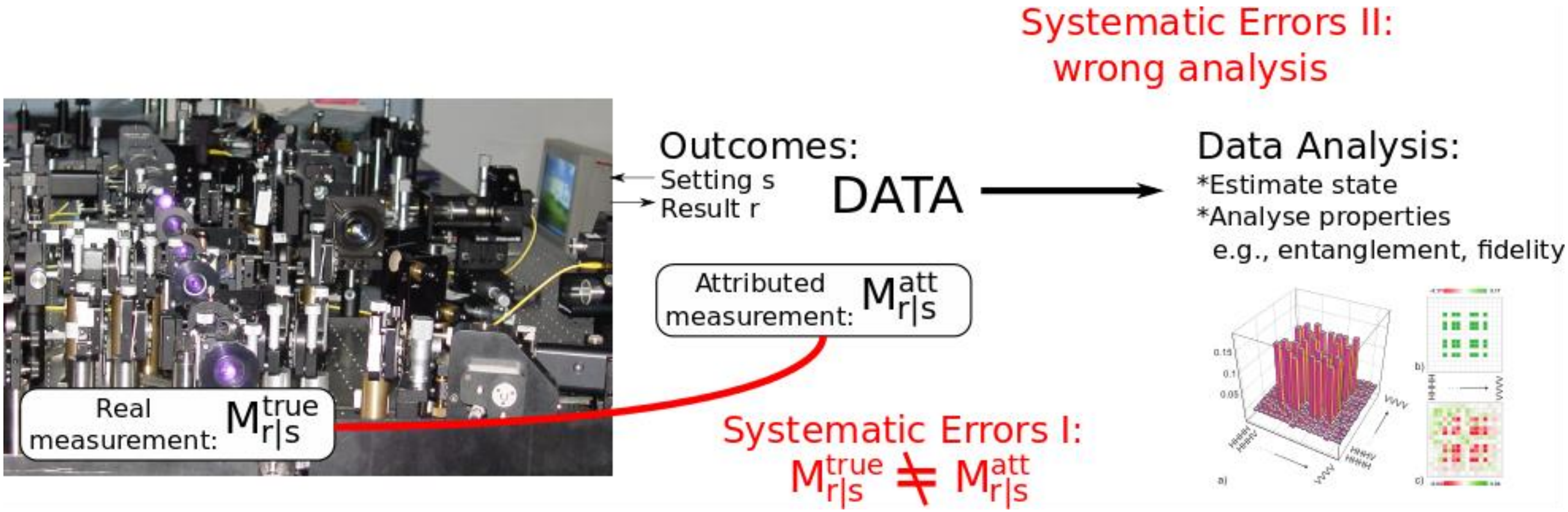

There are 2 types of **systematic errors:**

I.Deviations between real and attributed measurement description (due to misalignment, drifts, memory,...)

II.Errors in the classical analysis tool (wrong way to reconstruct the density operator)

Note that one has additionally statistical errors due to finite samples.

Systematic Errors – Results

Question: Are the observations at all compatible with the assumed description?

Two hypothesis tests:
a) Physicality witness
b) Likelihood-ratio test

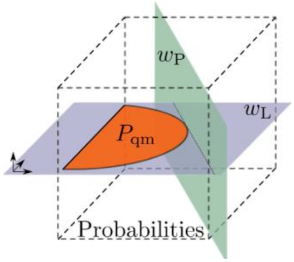

state	n	N_s	ϵ	w_L	w_P	LR
GHZ	4	750	0.20 *	97%	10^{-6}%	10^{-10}%
		750	0.12 *	100%	10^{-7}%	0.024%
		600	< 0.03	79%	81%	0.91%
Bell	2	61650	< 0.03	100%	100%	50%
SSSS	4	2600	< 0.03†	48%	84%	0.037%
BE	4	5200	< 0.03	99%	14%	35%
W	5	100	0.04	49%	91%	(0.081%)

* Cross-talk, † Laser fluctuation
Moroder *et al.* PRL 110, 180401

Question: Are properties deduced from the maximum likelihood/free least-squares state trustworthy?

No! Such estimates are biased, i.e., do not fluctuate around true value.

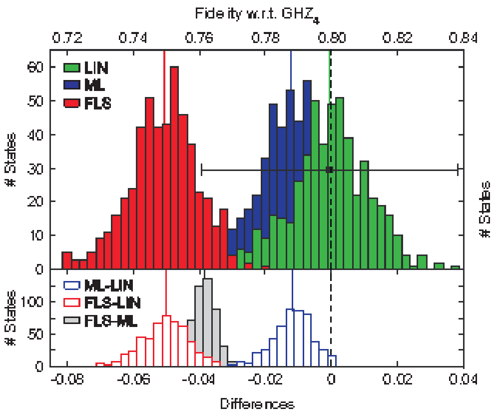

Wrong Fidelity!

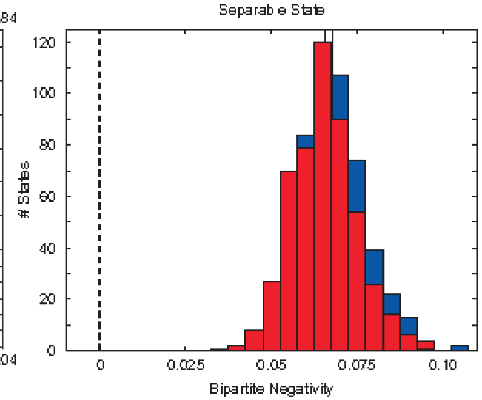

Fake entanglement

Solution: Linear evaluation similar to entanglement witnesses.
Schwemmer *et al.* arXiv.1310.8465

Efficient Tomography

QUASAR

- Permutationally invariant (PI) tomography
  - Suitable for PI states like e.g. GHZ, W or symmetric Dicke states
  - Measurement effort scales polynomially with the number of qubits
  - Scalable fitting algorithm based on convex optimization
- PI tomography of $D_6^{(3)}$, 28 settings (full tomomography 729)

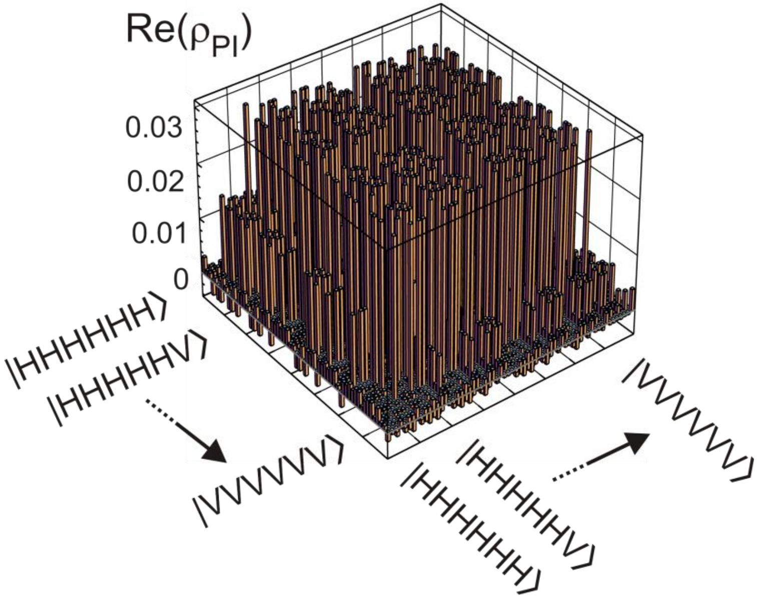

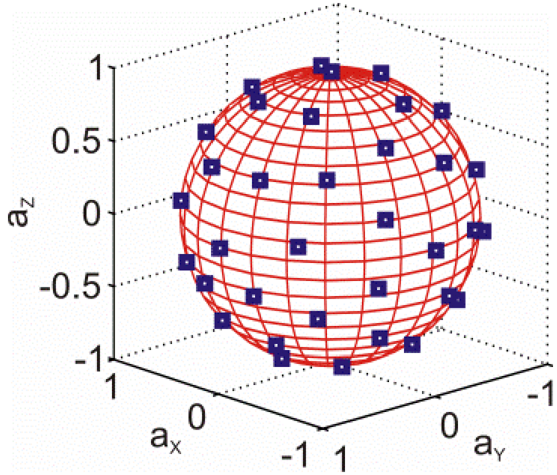

Measurement directions on the Bloch sphere

Efficient Tomography

QUASAR

- Combining PI tomography and compressed sensing
- Comparison of full, PI tomography and compressed sensing

State	Full	PI	CS	PI,CS
$\lvert D_6^{(0)}\rangle$	0.001	0.001	0.001	0.002
$\lvert D_6^{(1)}\rangle$	0.005	0.008	0.011	0.006
$\lvert D_6^{(2)}\rangle$	0.197	0.222	0.181	0.207
$\lvert D_6^{(3)}\rangle$	0.604	0.590	0.615	0.592
$\lvert D_6^{(4)}\rangle$	0.122	0.127	0.118	0.119
$\lvert D_6^{(5)}\rangle$	0.003	0.004	0.003	0.005
$\lvert D_6^{(6)}\rangle$	0.000	0.003	0.001	0.004
$\sum$	0.933	0.954	0.929	0.935

- Analysis of higher order noise at minimal effort
- PI witnesses enable fast entanglement detection

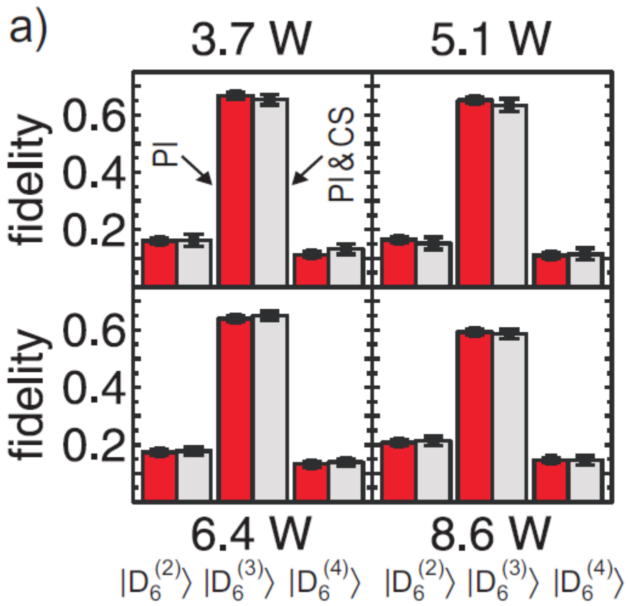

Multi-photon quantum interference with high visibility using multiport beam splitters

QUASAR

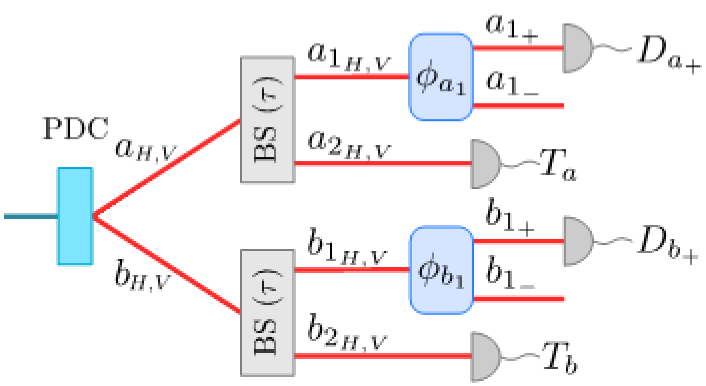

$$|\psi\rangle = \frac{1}{\cosh^2 K}\sum_{k=0}^{\infty}\tanh^k \sqrt{k+1}K|\psi^k\rangle$$

$$|\psi^k\rangle = \frac{1}{\sqrt{k+1}}\sum_{l=0}^{k}(-1)^k|l_H(k-l)_V,(k-l)_H l_V\rangle$$

Very inefficient linearly-responding detectors

$$p(D_{a+},D_{b+}|\varphi_i,\varphi_b) \sim \langle\psi|:N_a N_b:|\psi\rangle$$

Maximal Interference contrast

Idea: split signal on *M* mode multiports monitored by many detectors and take into account only single click events

$$V_2 = \frac{1}{1+2\tanh K}$$

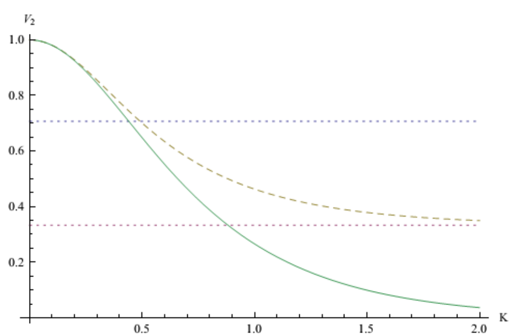

$$a_+ \to \frac{1}{\sqrt{M}}\sum_{j=1}^{M} a_{j+}$$

$$V_2^M = \frac{1-\frac{1}{M^2}\tanh K}{1+\frac{1}{M^2}\tanh K}$$

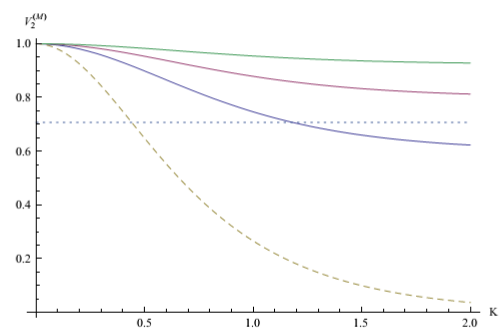

M. Stobińska, W. Laskowski, M. Wieśniak, M. Żukowski, Phys. Rev. A 87, 053828

Experimental Remote State Preparation

- Two-, four-. Or six-photon singlet states created from a common source
- Up to three-photons are sent to Alice, who performs local measurments on them
- The other photons are distributed among her partners,
- Depending on her projections, she can prepare a large class of states, including entangled ones

$$\{|0\rangle,|0\rangle\}\rightarrow|11\rangle$$

$$\{|0\rangle,|1\rangle\}\rightarrow\frac{1}{\sqrt{2}}(|01\rangle+|10\rangle)$$

$$\{|0\rangle,|0\rangle,|0\rangle\}\rightarrow|111\rangle$$

$$\{|0\rangle,|0\rangle,|1\rangle\}\rightarrow\frac{1}{\sqrt{3}}(|011\rangle+|101\rangle+|110\rangle)$$

$$\left\{|0\rangle,-\frac{1}{2}|0\rangle+\frac{\sqrt{3}}{2}|1\rangle,-\frac{1}{2}|0\rangle-\frac{\sqrt{3}}{2}|1\rangle\right\}\rightarrow$$

$$\frac{1}{2}(|001\rangle+|010\rangle+|100\rangle+|111\rangle)$$

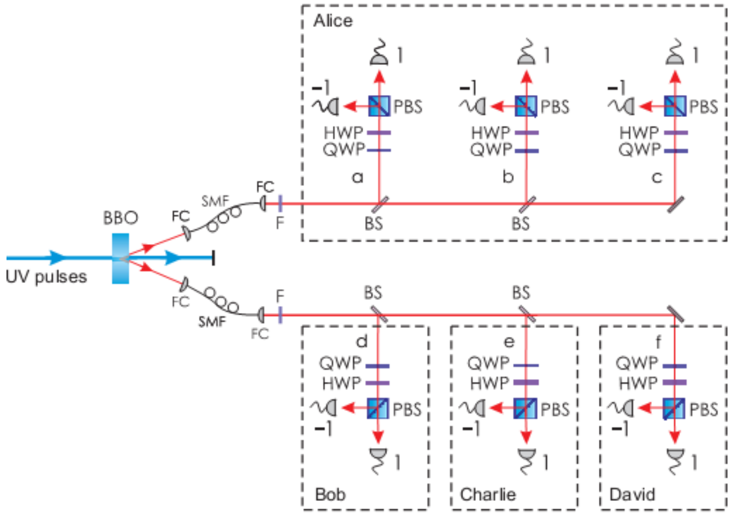

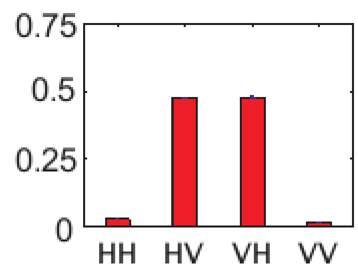

$$\frac{1}{\sqrt{2}}(|01\rangle+|10\rangle)$$

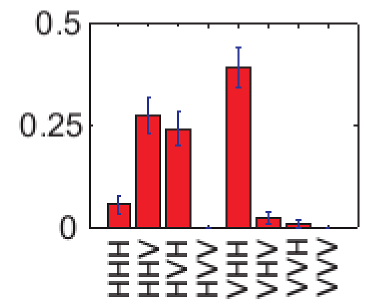

$$\frac{1}{\sqrt{3}}(|100\rangle+|100\rangle+|100\rangle)$$

M. Radmark, M. Wieśniak, M. Żukowski, M. Bourennane, Phys. Rev. A 88, 032304 (2013)

WP3 QU Metrology and Simulation

QUASAR

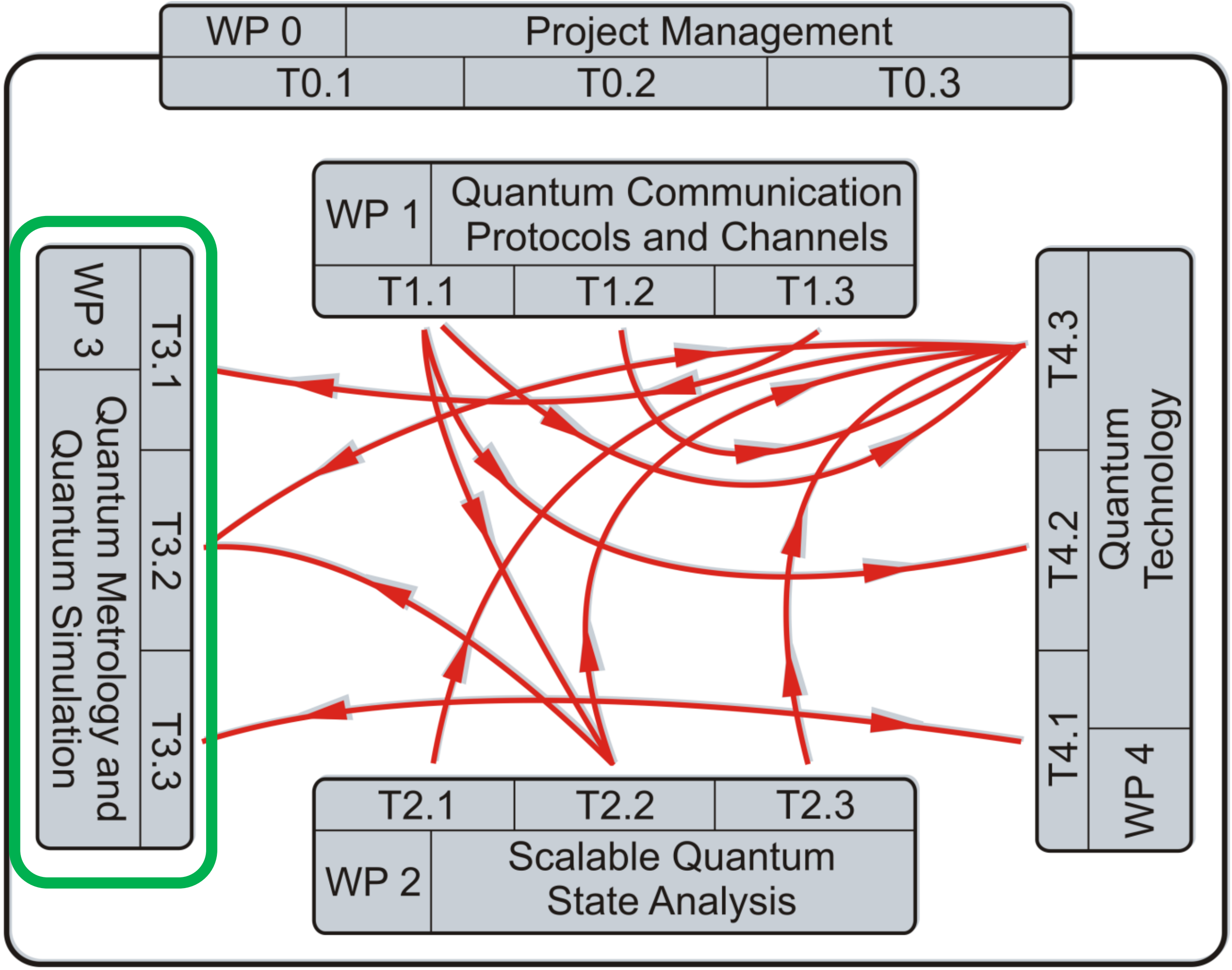

Bounds on quantum precision enhancement due to decoherence

QUASAR

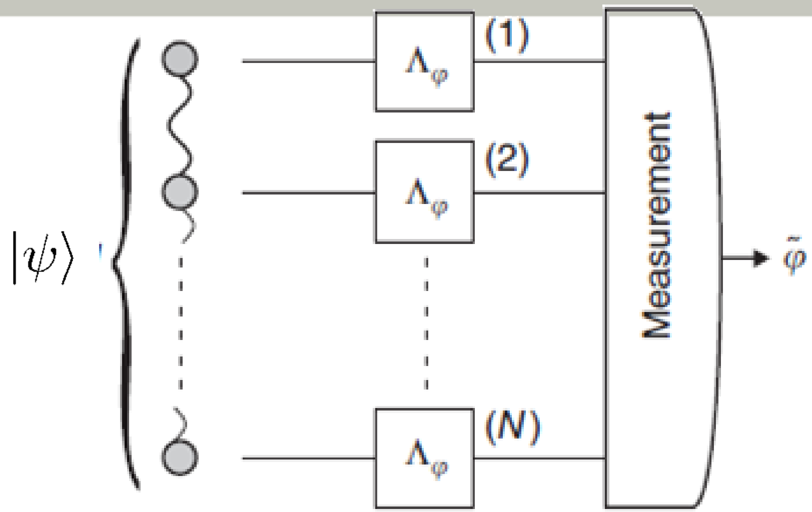

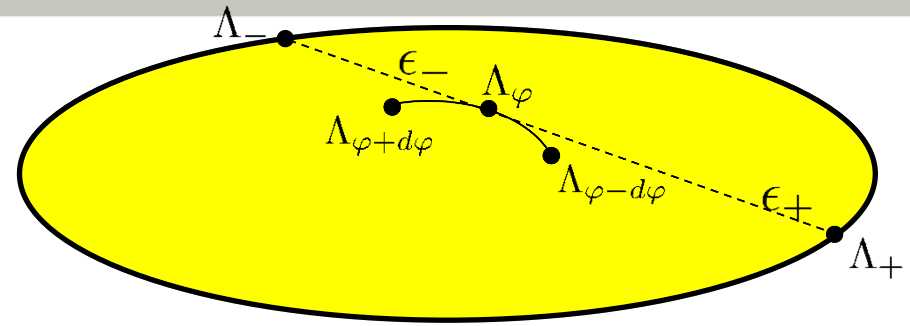

$$\Delta\varphi \geq \sqrt{\frac{\epsilon_+\epsilon_-}{N}} \qquad \Lambda_\pm = \Lambda_\varphi \pm \frac{d\Lambda_\varphi}{d\varphi}\epsilon_\pm$$

	Lossy interferometer	Dephasing	Depolarization	Spontaneous emission
$\Lambda_\varphi =$	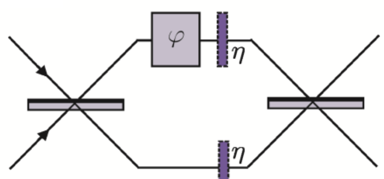	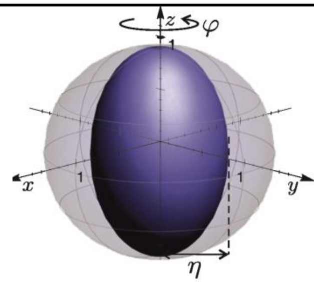	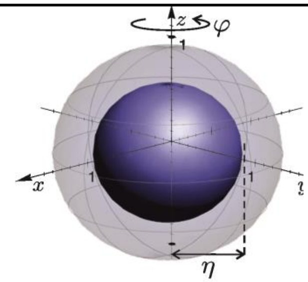	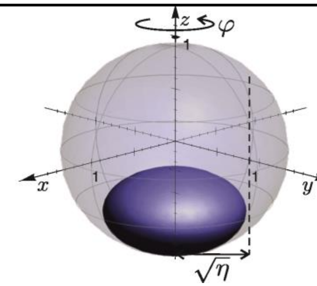
$\Delta\varphi \geq$	$\sqrt{\frac{1-\eta}{\eta}}\frac{1}{\sqrt{N}}$	$\frac{\sqrt{1-\eta^2}}{\eta}\frac{1}{\sqrt{N}}$	$\frac{\sqrt{(1-\eta)(1+3\eta)}}{2\eta}\frac{1}{\sqrt{N}}$	$\frac{1}{2}\sqrt{\frac{1-\eta}{\eta}}\frac{1}{\sqrt{N}}$

R. Demkowicz-Dobrzański, J. Kolodyński, M. Guta, Nat. Commun. **3**, 1063 (2012)

Matrix product states and quantum metrology

QUASAR

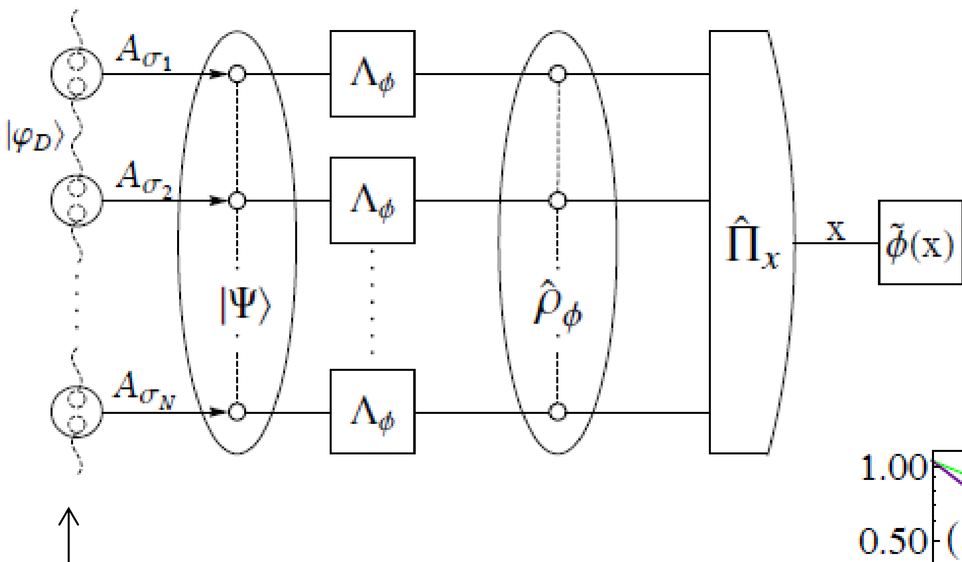

Matrix product state with bond dimension D

Low bond dimension matrix product states are sufficient.

$$\Delta\varphi = \frac{c}{\sqrt{N}}$$

No need to entangle strongly large number of probes

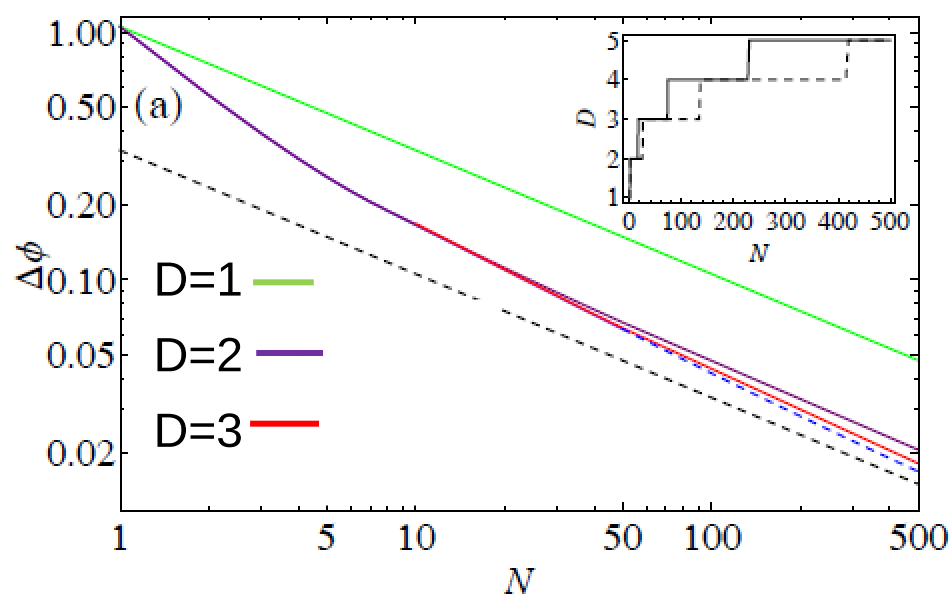

M.Jarzyna, R. Demkowicz-Dobrzanski, Phys. Rev. Lett. **110**, 240405 (2013)

Fundamental properties of the quantum Fisher information

QFI determines a lower bound on estimating *Θ*:

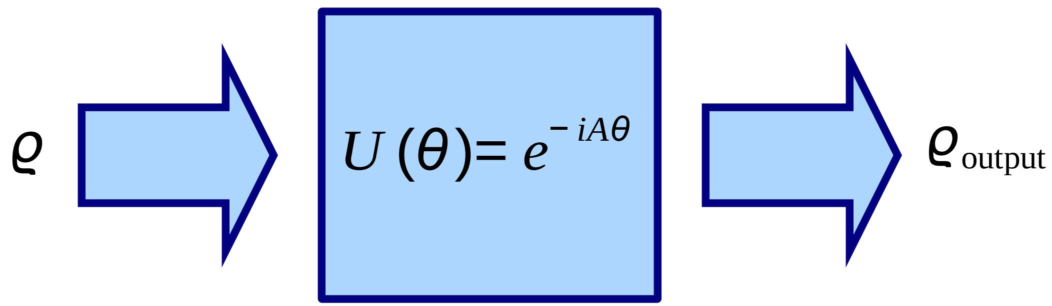

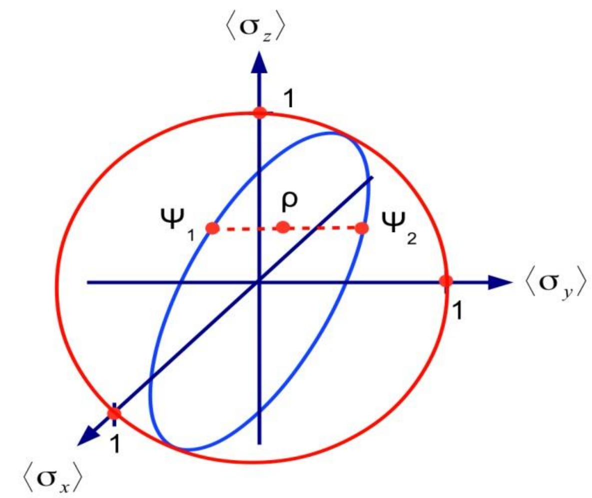

We have shown that it is its own convex roof and fulfills

$$\frac{1}{4}F_Q[\rho, A] \leq \sum_k p_k (\Delta A)^2_{\Psi_k} \leq (\Delta A)^2_\rho$$

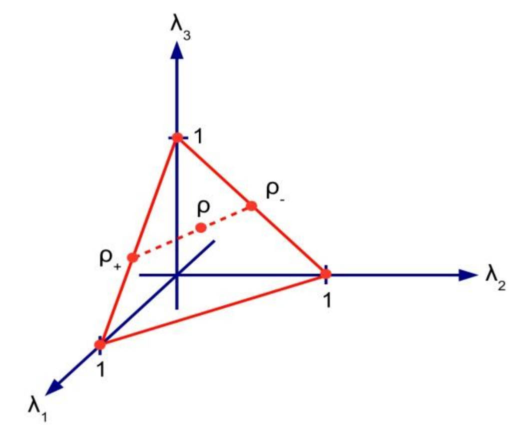

where the two bounds are tight. This paves the way

for estimating the QFI from measurements

[e.g., O.Gühne, Reimpell and M. Reimpell, R.F. Werner, Phys. Rev. Lett. (2007)].

G. Tóth and D. Petz, Phys. Rev. A **87**, 032324 (2013).

Metrology with macroscopic entangled states

A singlet state of 10^6-10^9 particles is created by spin squeezing (NJP 2010).

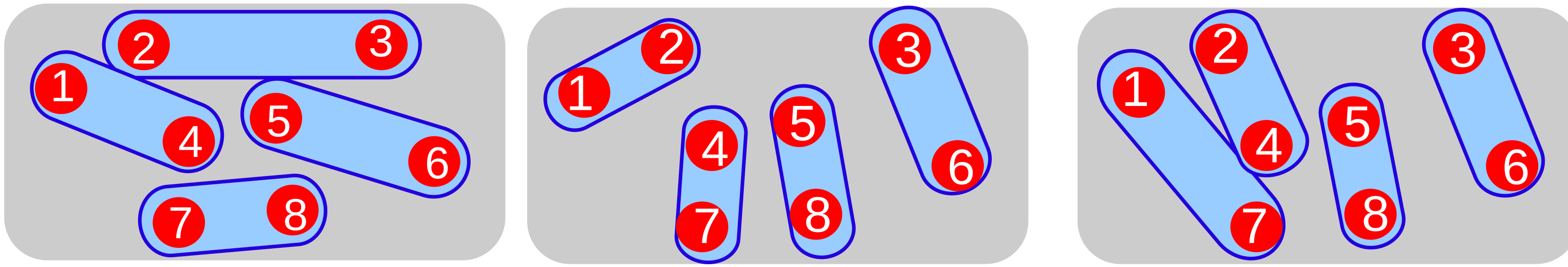

Singlets are sensitive to the gradient of the magnetic field.

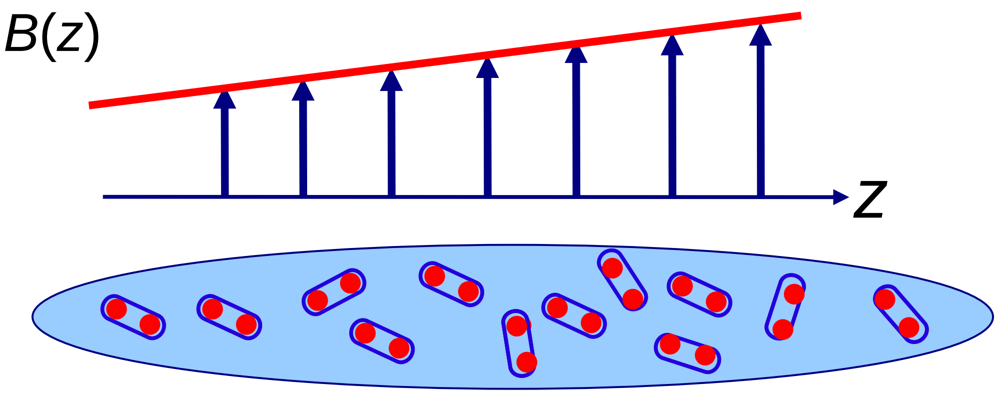

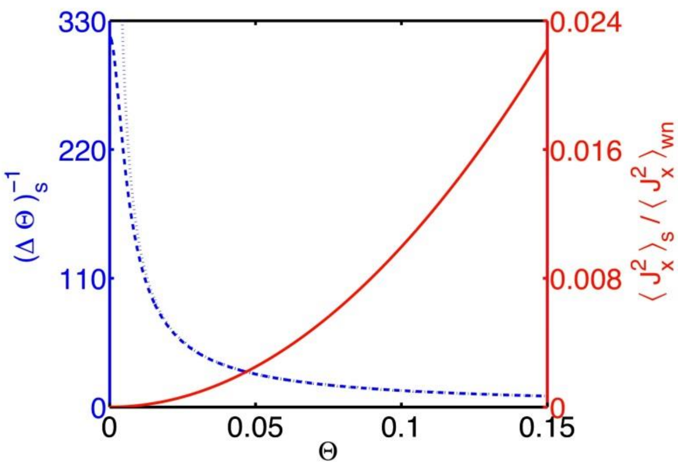

The gradient is estimated based on measuring the

Ongoing cold gas experiment at ICFO (M.W. Mitchell)

I. Urizar-Lanz, P. Hyllus, I.L Egusquiza, M.W. Mitchell and G. Tóth, Phys. Rev. A 88, 013626 (2013).

Quantum simulation of an interacting spin ring: the idea

QUASAR

The phase transitions of a 3-spin ring has been studied by a photonic quantum simulator encoding the wavefunction of the ground state by using a pair of entangled photons. The simulated magnetic field, leading to a critical modification of the correlation within the ring, is analysed by studying two- and three-spin entanglement. A quantitative connection between the violation of Svetlichny's inequality to the amount of three-tangle and tripartite negativity is performed.

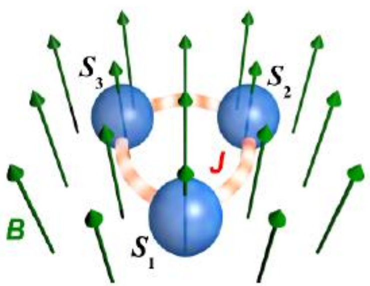

Three-spin Ising ring

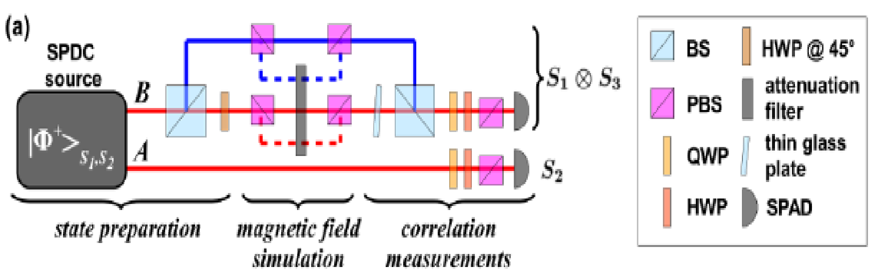

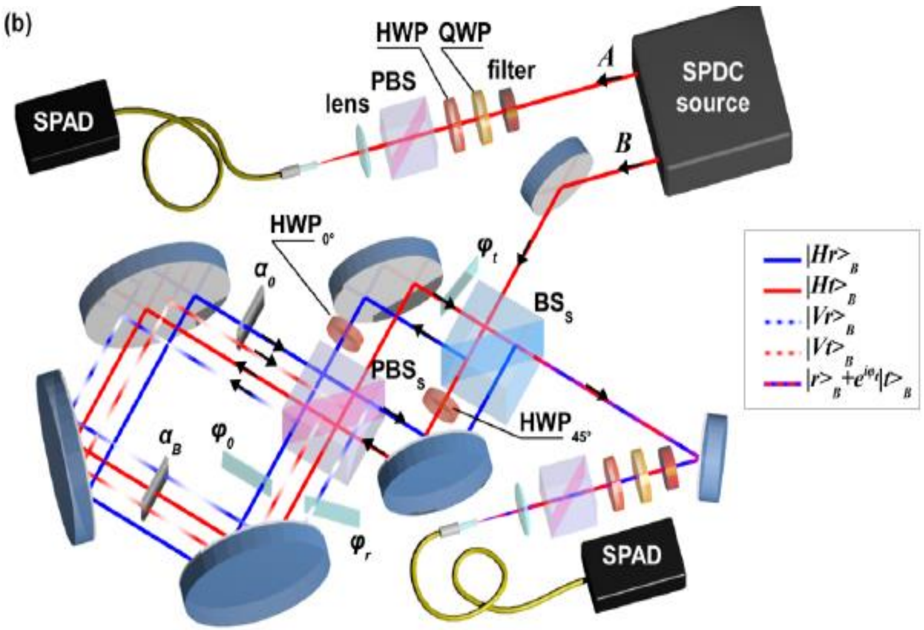

Experimental setup

A. Orieux *et al.*, *arXiv: 1312.1102v1* (2013)

Quantum simulation of an interacting spin ring: results

QUASAR

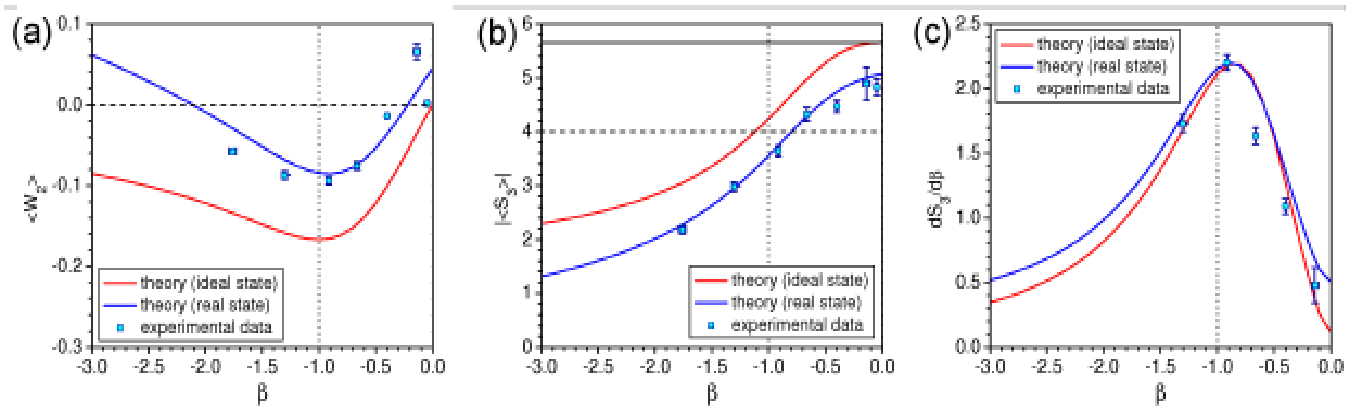

Measured evolution of the expectation value of (a) the bipartite entanglement witness <**W2**>, (b) the nonlocality Svetlichny function <**S3**> and (c) its derivative as a function of the magnetic field.The red line shows the theoretically expected evolution for the ideal ground state; and the blue line represents the theoretical evolution for a state affected by noise, as is the case in the experiment.

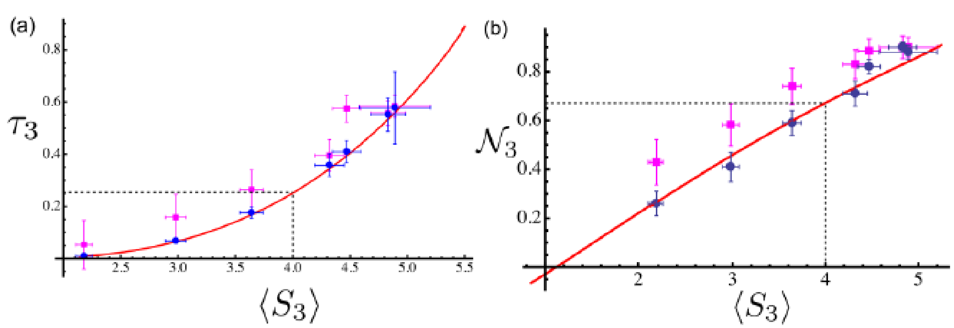

(a) Relation between the Svetlichny parameter <S3> and the three-tangle for the ground state of a three-spin Ising ring

WP4 Quantum Technology

QUASAR

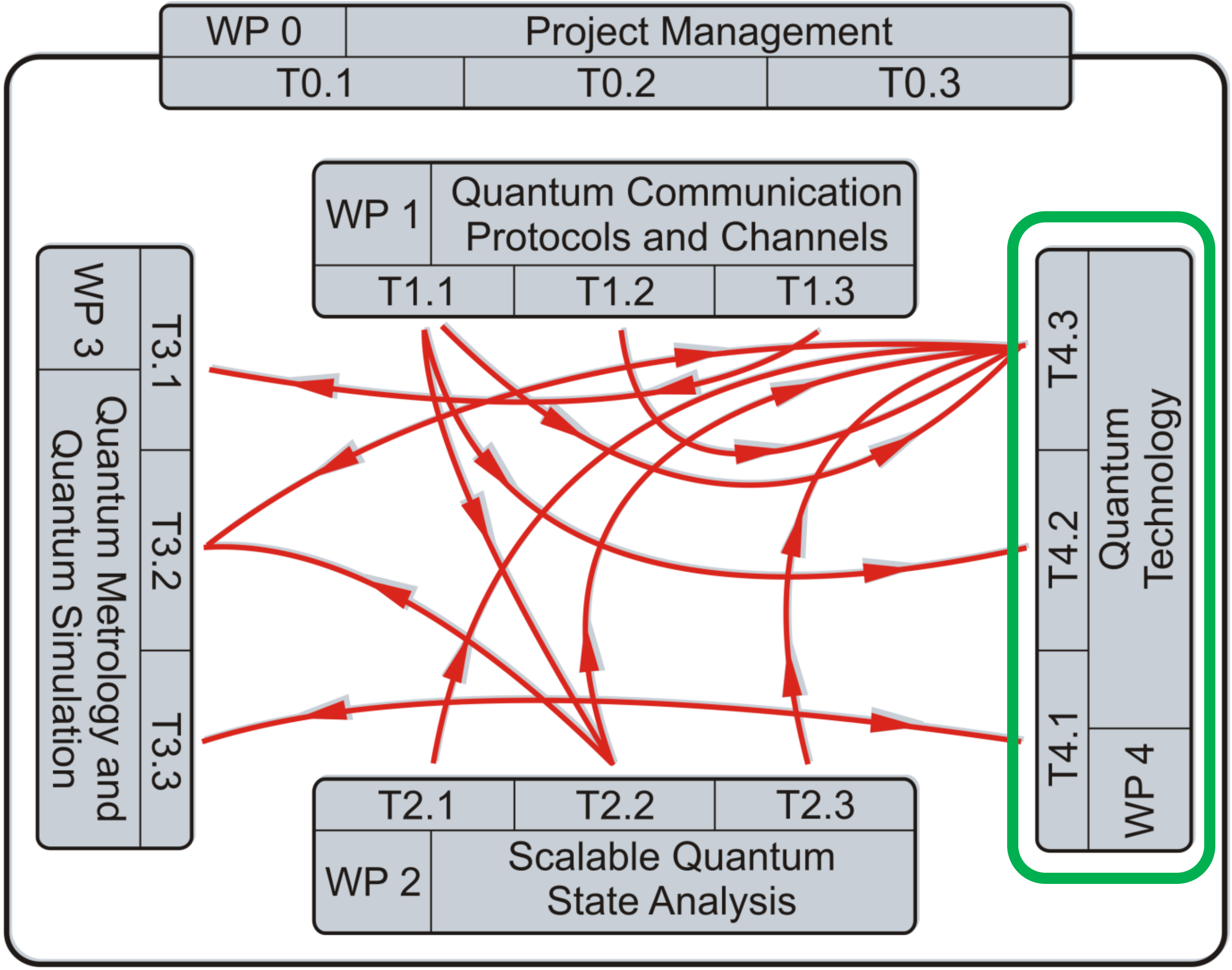

Parametric down-conversion in multimode nonlinear waveguides

QUASAR

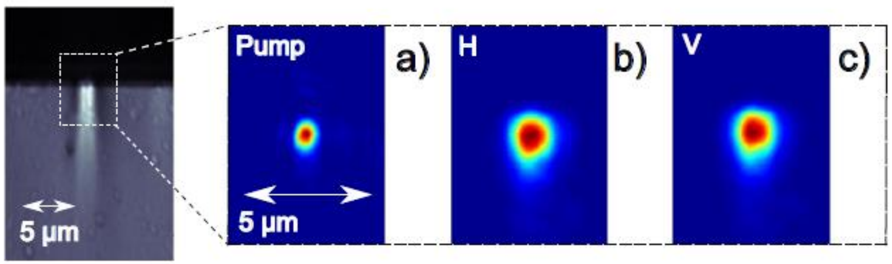

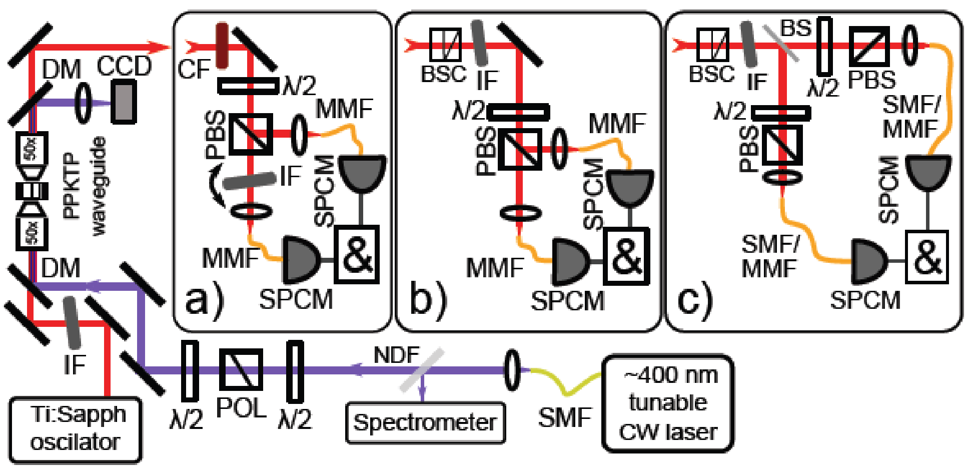

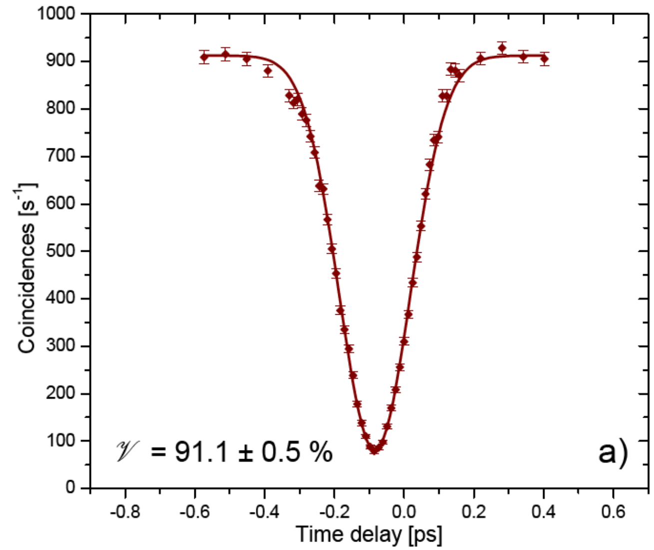

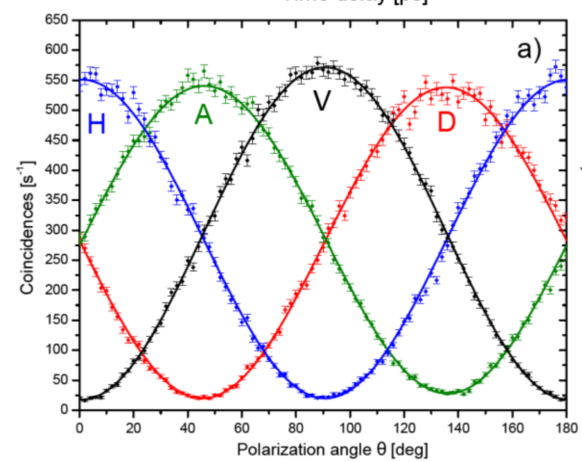

Integrated optical waveplates

QUASAR

Waveguide-based waveplates, fabricated by femtosecond laser pulses, have been realized to produce arbitrary single-qubit operations in the polarization encoding

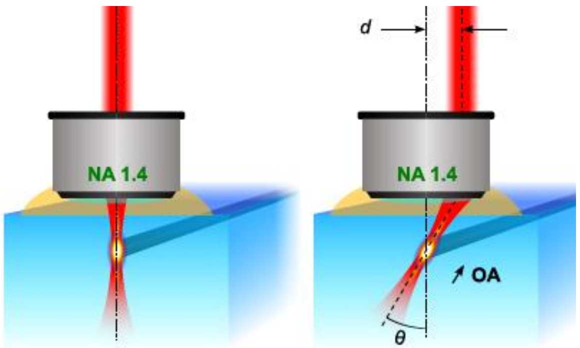

Using a high NA, oil-immersion objective and offsetting the writing beam before the objective results in a tilted elliptical waveguide with tuneable angle ❑

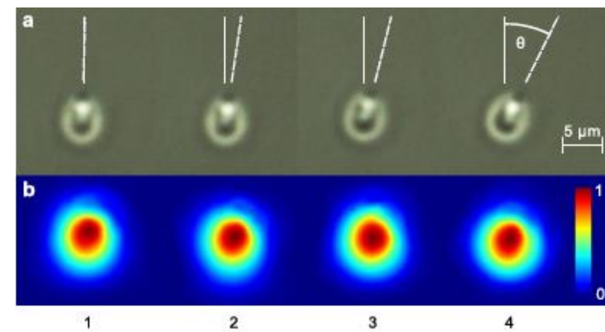

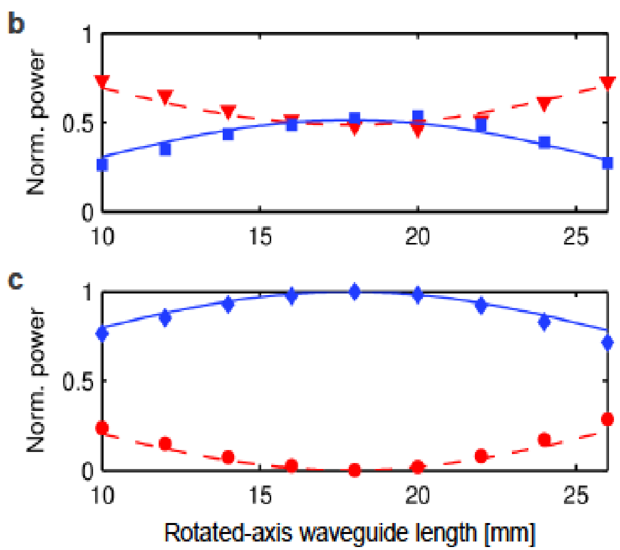

Characterization of a tilted waveplate with ❑ = 22.5°. Horizontally polarized input light: measured normalized power transferred into (**b**) the horizontal (red triangles)/vertical (blue squares) polarization states and (**c**) diagonal (blue diamonds)/antidiagonal (red circles) polarization states..

G. Corrielli *et al., arXiv: 1307.7541* (2013)

On-chip polarization analysis with integrated waveplates

QUASAR

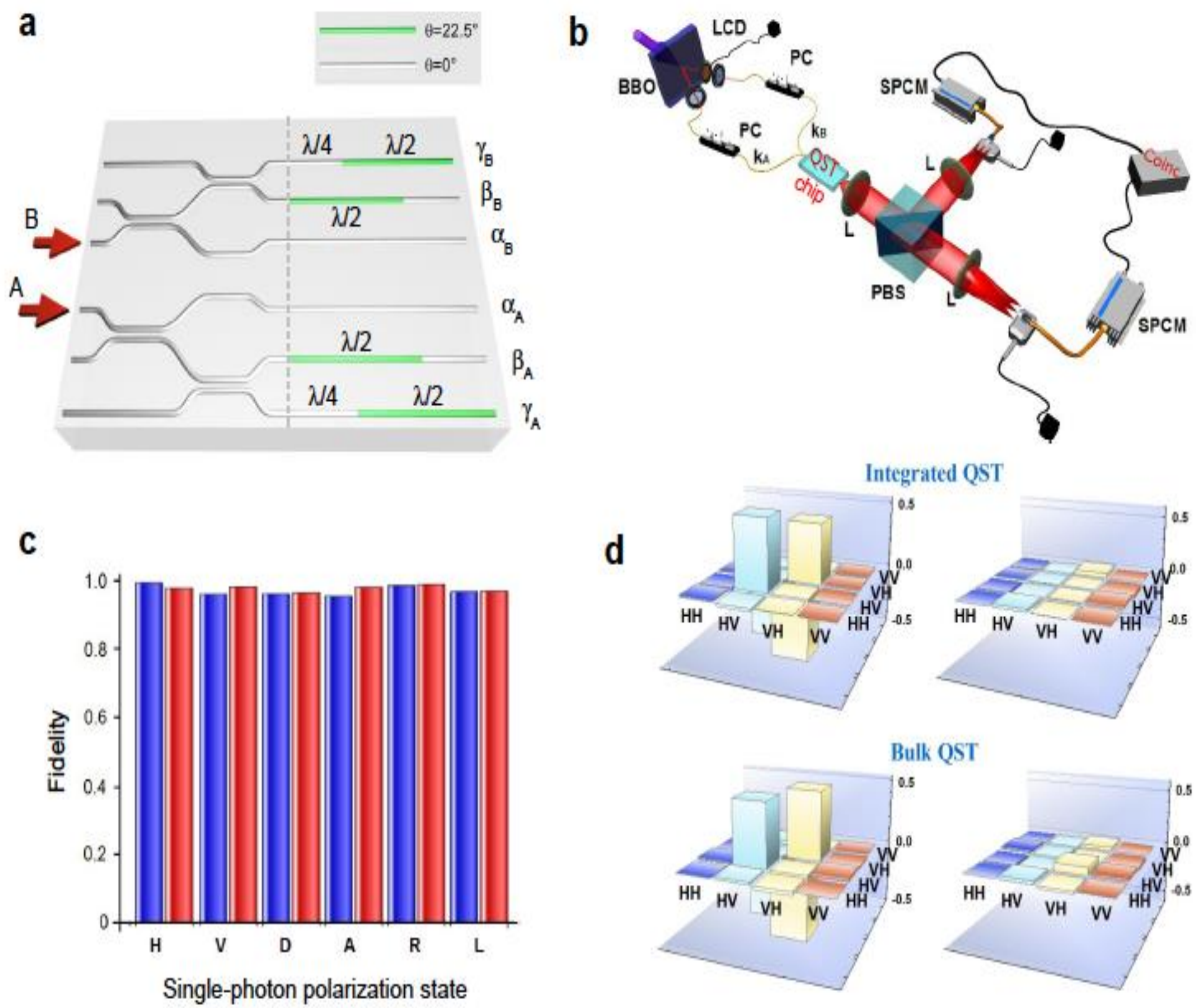

a): Scheme of the integrated device for quantum state tomography of a two-photon state. using integrated wps of suitable length and tilt, the two-photon state is prepared in the horizontal H/V, D/A and L/R bases by a single PBS. b): Experimental setup. c): Theoretical and experimental fidelities of different single photon states. d): Real and imaginary part of the reconstructed density matrix of the $|\Psi^{-}\rangle$ Bell state compared with the one realized by bulk optics.

G. Corrielli *et al., arXiv: 1307.7541* (2013)

Waveguide Writing Bench
Femtosecond-Laser Technology

QUASAR

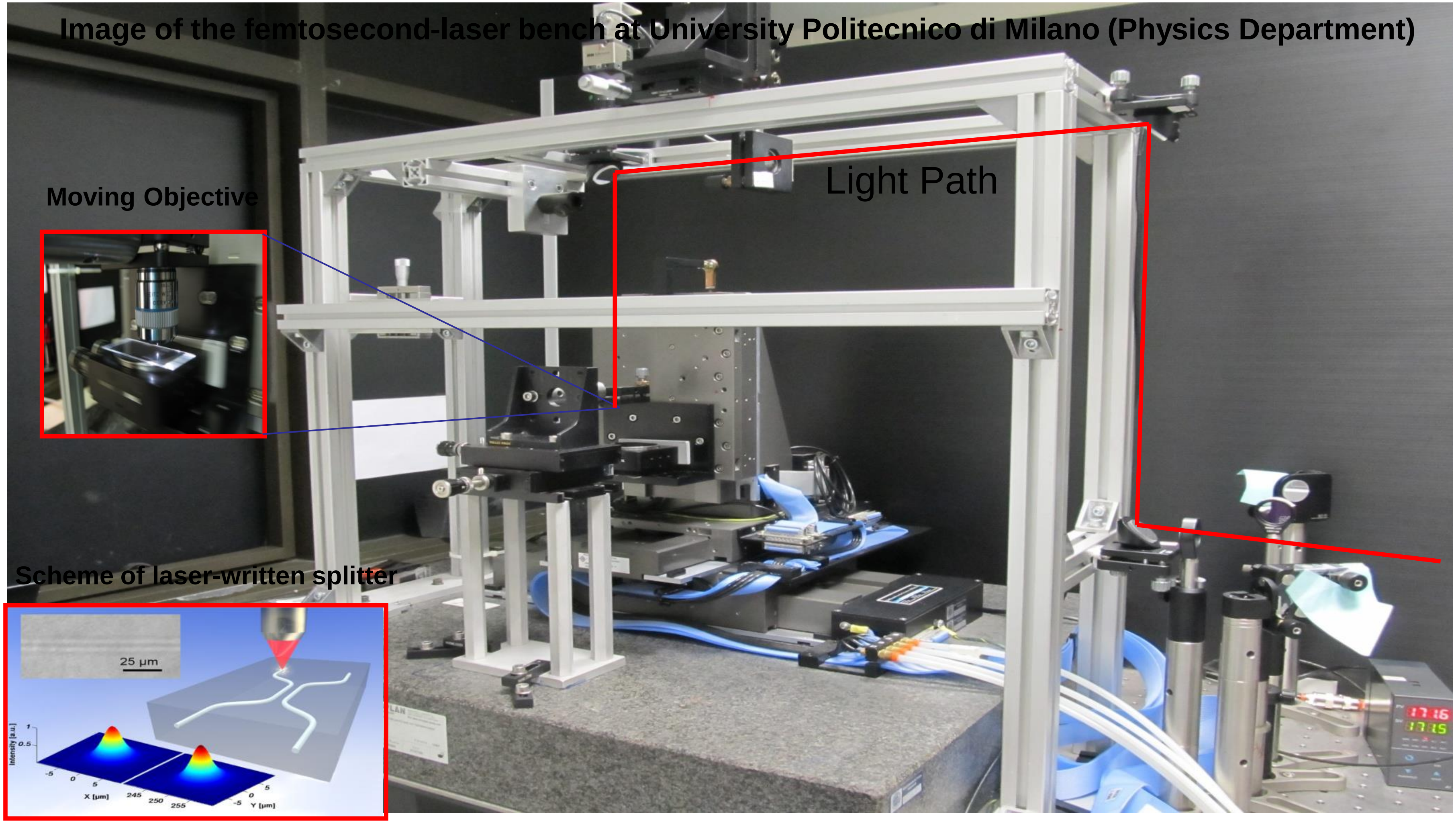

Stefano Pitassi, Riccardo Geremia (OPTOTEC SpA)

Theory of CNOT Quantum Gates
Glass Chip Layout

QUASAR

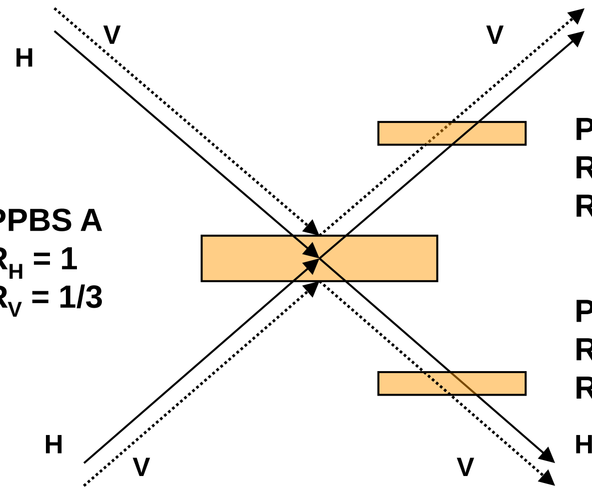

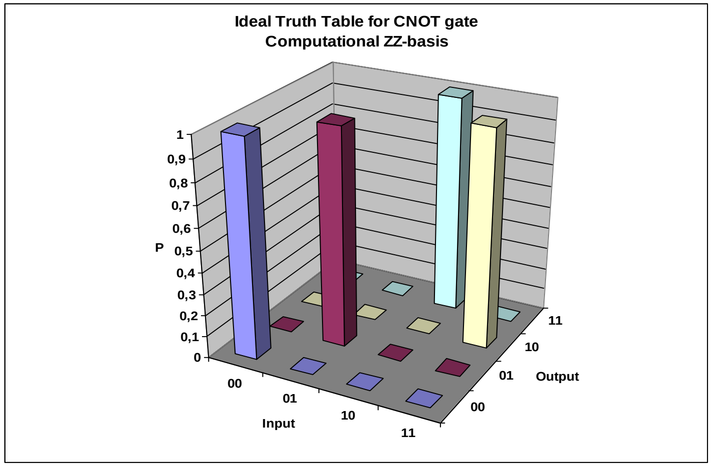

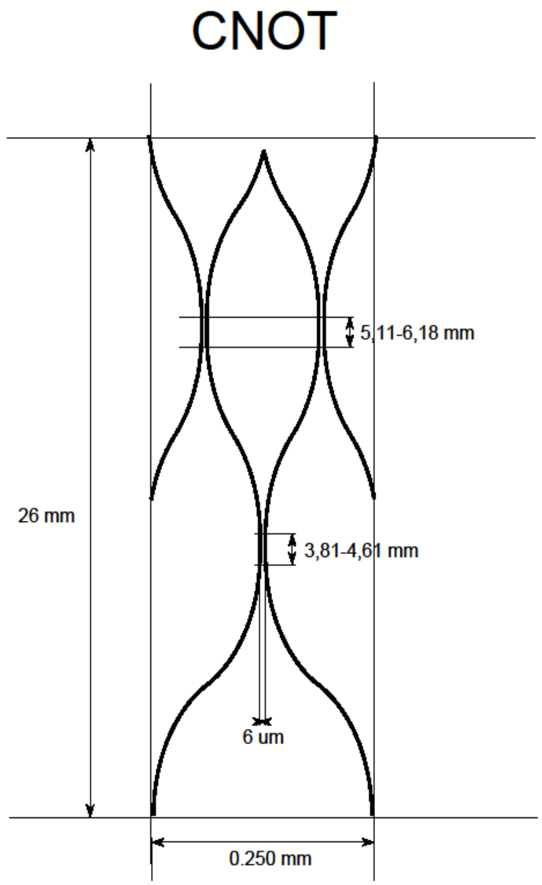

Waveguide Alignment
Fiber Pigtailing

QUASAR

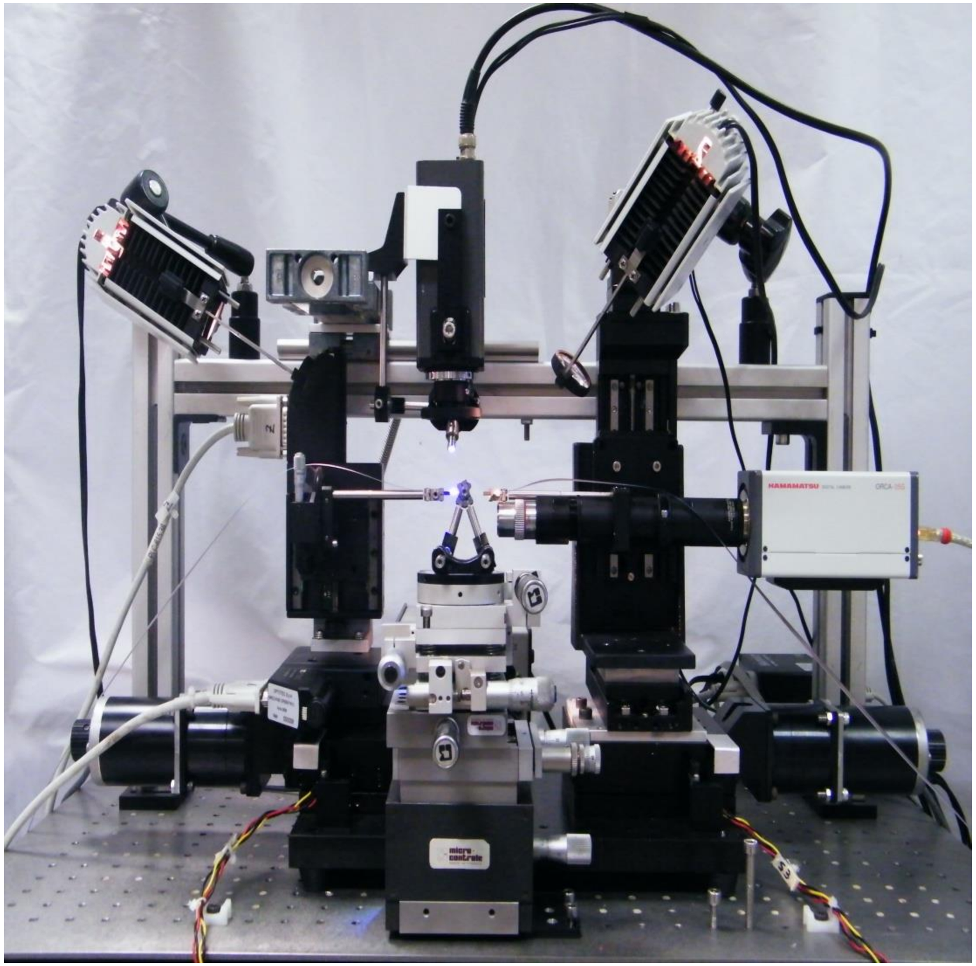

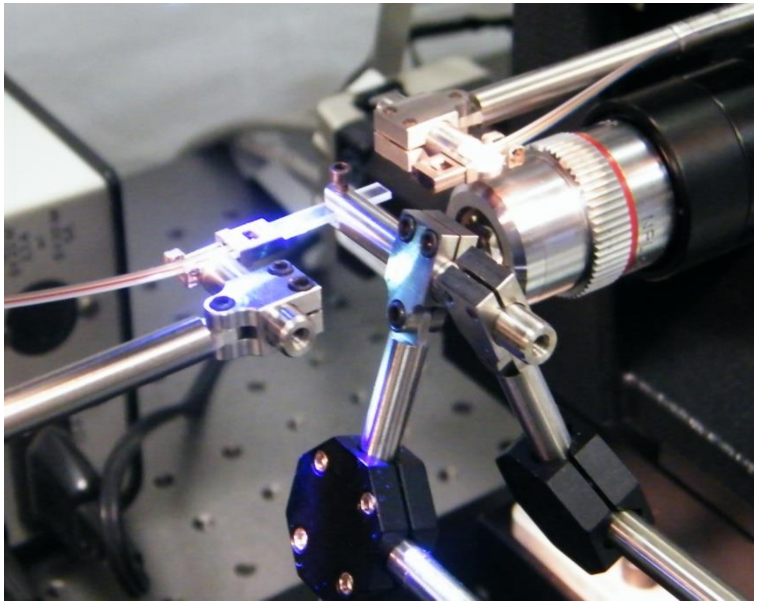

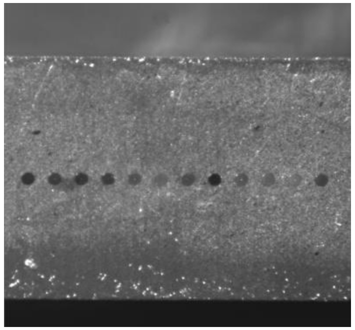

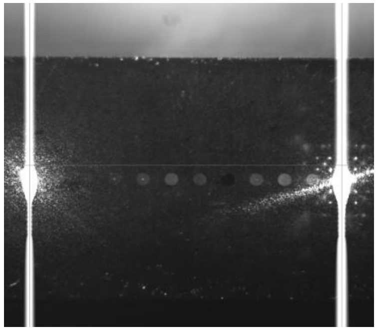

Stefano Pitassi (OPTOTEC SpA)

Device Packaging
Mechanical & Environmental Tests

QUASAR